Prmt5 promotes vascular morphogenesis in zebrafish independently of its methyltransferase activity.

Aurelie Quillien[1*], Manon Boulet[1,2], Severine Ethuin[1], Laurence Vandel[1,2*]

[1]Centre de Biologie du Développement (CBD), Centre de Biologie Intégrative (CBI), Université de Toulouse, CNRS, UPS, France

[2]Current affiliation : Université Clermont Auvergne, CNRS, Inserm, GReD, Clermont-Ferrand, France

*Corresponding Authors

Aurélie Quillien (aurelie.quillien@gmail.com)

Laurence Vandel (laurence.vandel@uca.fr)

ABSTRACT

In vertebrate, blood cell formation is tightly associated with the development of the vascular system. While the transcriptional cascade underlying blood vessel formation starts to be better characterized, little is known concerning the role and mode of action of epigenetic enzymes during this process.

Here, we explored the role of the Protein Arginine Methyl Transferase Prmt5 during blood vessel formation and in hematopoiesis in zebrafish. Through the generation of a Prmt5 mutant, we highlight a key role of Prmt5 in both hematopoiesis and blood vessel formation. Prmt5 promotes vascular morphogenesis through the transcriptional control of ETS transcription factor and adhesion proteins in endothelial cells. Moreover, we show that the methyltransferase activity of Prmt5 was not required to regulate gene expression, and comparison of chromatin architecture impact on reporter genes expression lead us to propose a role of scaffold protein for Prmt5 to facilitate chromatin looping formation in these cells.

Key words

Prmt5; zebrafish; angiogenesis; hematopoiesis; endothelial cells; chromatin looping

INTRODUCTION

In vertebrate, blood cell formation is tightly associated with the development of the vascular system. Hematopoietic Stem Cells (HSC) which give rise to the different blood cell lineages emerge directly from the ventral part of the dorsal aorta, an area referred to as the hemogenic endothelium. VEGF (Vascular Endothelial Growth factor) signaling is crucial for the formation of both tissues, as animals deficient for VEGFA or VEGFR2 exhibit a lack of blood cells and vasculature and die prematurely (Carmeliet et al., 1996; Shalaby et al., 1997; Covassin et al., 2009, 2006). ETS transcription factor ETV2 functions as a master regulator for the formation of endothelial and hematopoietic cell lineages through the induction of both transcriptional programs (Wong et al., 2009, Liu et al 2015). In endothelial cells, ETV2 regulates the expression of other ETS transcription factors, VEGF signaling receptors and effectors, Rho-GTPases and adhesion molecules (Wong et al., 2009, Liu et al 2015). Adhesion molecules have been shown to be crucial players for vascular morphogenesis. For instance, Vascular Endothelial cadherin (VE-cad/ cdh5) and endothelial cell-selective adhesion molecule (Esama) are essential for junction remodeling and blood vessel elongation in zebrafish (Sauteur et al 2014, 20117). Indeed, loss of function of both *cdh5* and *esama* leads to the formation of disconnected vessels and delayed lumen formation. Likewise, knock down of the scaffold protein Amolt2 which associates to VE-cadherin also leads to sprout elongation defects and narrowed aortic lumen (Hultin et al, 2014). While the transcriptional cascade underlying blood vessel formation starts to be better characterized, little is known concerning the role and mode of action of epigenetic enzymes during this process. While the role of chromatin-modifying enzymes has been described as central in cardiovascular disease and development (Rosa-Garrido et al. 2018, Shailesh et al 2018), only few examples illustrate in detail the role of epigenetic enzymes during blood vessel development. For instance, the chromatin-remodeling enzyme BRG1 affects early vascular development as well as hematopoiesis in mice (Griffin et al. 2008). The histone acetyltransferase P300 has been proposed to be recruited at the promoter of specific endothelial genes by the ETS transcription factor ERG (ETS Related Gene) to control gene expression both *in vivo* in zebrafish and in HUVEC (Human Umbilical Vein Endothelial Cell) (Fish et al 2017; Kalna et al 2019).

Given the common origin of blood and endothelial cells, and their partially shared transcriptional programs, it is plausible that known chromatin-modifying enzyme affecting hematopoiesis could also perturb blood vessel formation. Along this line, the epigenetic enzyme Prmt5 (Protein Arginine Methyltransferase 5) has been identified as a key player in blood cell formation (Liu et al 2015) but its impact in endothelial development has not been investigated to date. Prmt5 catalyzes the symmetric di-methylation of arginine on a wide variety of proteins including histones and therefore acts on many cellular processes such as, genome organization, transcription, differentiation, cell cycle regulation or spliceosome assembly among others (Blanc and Richard, 2017; Stopa et al., 2015; Karkhanis et al, 2011). Prmt5 is mainly known to repress transcription through the methylation of arginine residues on histones H3 and H4. Prmt5 has been shown to regulate several differentiation processes such as myogenesis, oligodendrocyte and germ cell differentiation or hematopoiesis (Shailesh et al 2018, Batut et al., 2011, Zhu et al. 2019, Liu et al 2015). In mice, *prmt5* knock out is embryonic lethal as it prevents pluripotent cells to form from the inner cell mass (ICM) (Tee et al., 2010). Conditional loss of *prmt5,* leads to severe anemia and pancytopenia in mice and Prmt5 maintains HSC as well as ensures proper blood cell progenitor expansion (Liu et al 2015). The loss of *prmt5* leads to oxidative DNA damages, increased cell apoptosis due to p53 dysregulation and as a consequence, to HSC exhaustion. In this context, Prmt5 protects HSC from DNA damages, by allowing the splicing of genes involved in DNA repair that are particularly sensitive to these damages (Tan et al 2019).

Here, we explored the role of the Protein Arginine Methyl Transferase Prmt5 during blood vessel formation and in hematopoiesis in zebrafish. Through the generation of a Prmt5 mutant, we highlight the key role of this gene during vascular morphogenesis *via* the control of expression of several ETS transcription factors and adhesion molecules. Moreover, we show that Prmt5 methyltransferase activity is not required for blood vessel formation and propose that Prmt5 helps to shape correct chromatin conformation in endothelial cells.

RESULTS

Prmt5 is required for HSC maintenance and lymphoid progenitor expansion

To characterize *prmt5* function, we generated a *prmt5* mutant by targeting the second exon of *prmt5* with the CRISPR/Cas9 system. A deletion of 23 nucleotides was obtained, leading to a premature stop codon before the catalytic domain of Prmt5 (Fig. 1A). As a consequence, Prmt5, which was expressed ubiquitously in the trunk at 24hpf, was no longer detected in the mutant (Fig. 1B, C). Similarly, Prmt5 expression was severely reduced in *prmt5* morpholino-injected embryos (Batut et al. 2011) as compared to control morphants (Fig. S1 A, B). In order to test whether Prmt5 regulates hematopoiesis in zebrafish in a similar way as in mouse, we took advantage of the transgenic line *Tg*(*gata2b:Gal4;UAS:lifeactGFP)* that labels Hematopoietic Stem Cells (HSC) that are positive for *gata2b* (Butko et al. 2015). HSCs emerge from the ventral wall of the dorsal aorta (DA, Fig. 1D-F'), before migrating into the Caudal Hematopoietic Tissue (CHT) (Fig. 1D) where Hematopoietic Stem and Progenitor Cells (HSPCs) proliferate and undergo maturation (Butko et al. 2015). In agreement with the data published in mice (Liu et al, 2015), the loss of *prmt5* led to an increased number of *gata2b*+ HSCs in 36 hpf mutant embryos as compared to wild type ones (Fig. 1E-G). In addition, we found that the relative expression of *scla*, *runx1* or *cmyb* that are specifically expressed in emerging HSCs was increased in *prmt5* mutant embryos as compared to wild type embryos (Fig. 1H). These results suggest that Prmt5 regulates the number of emerging HSCs from the dorsal aorta. We next investigated whether blood cell formation was impaired in *prmt5* zebrafish mutant as described in mouse (Liu et al, 2015). HSPCs give rise to different blood cell progenitors, such as lymphoid progenitors which colonize the thymus leading to T lymphopoiesis (Fig. 1D) (Ma et al, 2013). As *gata2b*+ lymphoid progenitors deriving from *gata2b*+ HSCs, can be detected in the thymus of transgenic zebrafish larvae at day 3 (Butko et al. 2015), we investigated whether Prmt5 could act on theses progenitors. Indeed, we found that at 5 days, the number of *gata2b*+ *lymphoid* progenitors in the thymus was significantly reduced in *prmt5* mutant embryos as compared to wild type embryos (Fig. 1I-K), suggesting

that Prmt5 is required for hematopoietic progenitor expansion. Altogether, these data indicate an important and conserved role of Prmt5 during hematopoiesis in zebrafish as in mouse.

Prmt5 is required for vascular morphogenesis

As Prmt5 regulates zebrafish hematopoiesis, we next wanted to know whether Prmt5 could also play a role during blood vessel formation, either during angiogenesis or vasculogenesis. First, we analyzed the expression and localization of Prmt5 by immunostaining in *Tg(fli1a:eGFP)* transgenic embryos, in which endothelial cells can be visualized with *egfp* (Lawson and Weinstein 2002). We found that Prmt5 was expressed ubiquitously, and in early endothelial cells at 14 somite stage (Fig. 2A-A''). At 24 hpf, Prmt5 was expressed in endothelial cells of the dorsal aorta (DA) and of the cardinal vein (CV) (Fig. 2B, B', D). Prmt5 was also expressed in Intersegmental Vessels (ISVs) sprouting from the DA, in either the tip cell (leading the sprout) or the stalk cell (Fig. 2C, C', D). We then analyzed whether blood vessel formation was affected in transgenic *Tg(fli1a:eGFP) prmt5* mutants at 28 hpf. Dorsal aorta diameter of mutant embryos was reduced as compared to the control (Fig. 2D, E, F close-ups), suggested that lumen formation was perturbed in the mutant context. To further confirm this result, we took advantage of the Notch reporter line *Tg(TP1bglob:VenusPEST)*^{s940} in which only the dorsal aorta cells expressed the transgene while cardinal vein endothelial cells did not (Ninov et al, 2012, Quillien et al, 2014). In this transgenic context the area occupied by the dorsal aorta in *prmt5* morphant embryos was significantly reduced as compared to control embryos (Fig. 2G-I). *Prmt5* mutant embryos also showed a defect of sprouting ISV to reach the most dorsal part of the trunk and to connect with other ISVs to form the Dorsal Longitudinal Anastomotic Vessel (DLAV) (Fig. 2D, E, F). This defect was due to a reduction of ISV length compared to wild type embryos (Fig. 2E, F, K) without any impact on the number of endothelial cells (Fig. 2J). The observed size reduction of ISVs is thus most likely the result of an elongation issue rather than a proliferation defect. Of note, *prmt5* morphants reproduced the phenotype observed in *prmt5* mutants *i.e* a reduced ISV length at 28 hpf as well as a slight

decrease in the number of endothelial cells, thus validating our data by an alternative approach (Fig. S1 C-F).

To get a better insight into the impact of Prmt5 on the dynamics of vascular, we performed and compared time-lapse analyses in control with *prmt5* morphant embryos. Time-lapse confocal movies were carried out from 28 hpf to 38 hpf to follow the elongation of ISVs to the formation of an effective lumen. As compared to control morphants, if *prmt5* morphants exhibited a normal extension of ISVs, ISV lumen formation was impaired as well as the DLAV formation. Indeed, *in prmt5* morphants tip cells failed to stay connected to the stalk cells and to contact other tip cells to allow the formation of the DLAV (Fig. 3A-B). Moreover, supernumerary connections were detected in the context of *prmt5*-loss of function (Fig. 3B). Altogether, these data suggest a central role for Prmt5 in vascular morphogenesis.

The master gene regulator ETV2, ETS transcription factors and adhesion proteins have been shown to be involved in blood vessel formation (Pham et al. 2007, Craig et al. 2015, Hultin et al, 2014, Sauteur et al. 2014, Sauteur et al. 2017). To test whether Prmt5 could regulate the expression of these genes, we performed qPCR experiments on mutant embryos and on their wild type counterparts. While we found that *etv2* expression was not affected by the loss of *prmt5*, expression of ETS transcription factors (*fli1a, fli1b*) and adhesion proteins *(cdh5*, *agtr2*, *esama* and *amotl2a)* all known ETV2 target genes (Wong et al., 2009), was significantly reduced in *prmt5* mutant (Fig. 3C). As *etv2* expression was unaffected by the loss of *prmt5* but its targets were down-regulated, it is tempting to speculate that Prmt5 could modulate the activity of ETV2 at post-translational level.

Prmt5 methyltransferase activity is not required for vascular morphogenesis

That Prmt5 modulates gene expression by methylating a variety of proteins including histones but also transcription (co)factors among others led us to test whether Prmt5 methyltransferase activity was required for vascular morphogenesis. To this end, *prmt5* mutant embryos were injected with wild type *human prmt5* mRNA (*hprmt5WT*) or with a catalytic mutant form of this

mRNA (*hprmt5MUT*) (Pal et al 2003) and ISVs elongation as well as expression of *etv2* target genes were analyzed. Surprisingly, both mRNAs were able to restore ISV elongation as indicated by the average ISV length in injected mutant embryos compared to non-injected mutant ones (Fig. 4A-E). We observed that the average length of ISVs in *hprmt5WT* injected mutants was even longer than intersegmental vessels of wild type embryos while the average length in *hprmt5MUT* injected mutants was significantly superior to non-injected mutants but shorter than control embryos (Fig. 4 E). Moreover, we did not notice any difference in the cell number per ISV in the different contexts (Fig. 4F). These results suggest that, despites to a different extend, both mRNAs were able to rescue the loss of *prmt5* function, suggesting that the methyltranferase activity of Prmt5 is mostly dispensable for Prmt5 function in blood vessel formation. Moreover, expression level analysis of *etv2* target genes by qPCR revealed that at the exception of *fli1a*, expression of all of them was restored similarly by injecting either *hprmt5WT* or *hprmt5MUT* mRNAs (Fig. 4G).

Prmt5 might help to shape correct chromatin conformation in endothelial cells

As Prmt5 methyltransferase activity seems not to be required for gene expression regulation in vascular morphogenesis, we can speculate that Prmt5 could play the role of a scaffold protein in complexes mediating transcription and chromatin looping. Indeed, Prmt5 has been proposed to promote enhancer-promoter looping at the PPARγ2 locus and more broadly to facilitate chromatin connection in adipocytes, *via* the recruitments of Mediator subunit MED1 and of SWI/SNF chromatin remodeling complex subunit Brg1 ATPase (Leblanc et al., 2016). Thus, we decided to inspect the chromatin architecture of the flanking region of identified Prmt5 regulated genes using ATAC-seq data from zebrafish endothelial cells that we previously generated (Quillien et al., 2017). Doing so, we found that all regulated genes, at the exception of *fli1a*, contained at least one putative enhancer distant at minima of 6kb from the TSS (Fig. S2 A-F) indicating that their expression could rely on proper chromatin looping. In order to gain insight into a potential role of Prmt5 in supporting proper chromatin conformation in endothelial cells, we decided to analyze the expression of *Gal4* reporter gene in an endogenous and an

artificial chromatin context (Fig. 5A-E). The first construction was the transgenic line *TgBAC(cdh5:GAL4FF);Tg(UAS:GFP)* that contained the sequence of an optimized version of Gal4VP16 (*GAL4FF*) inserted at the transcription start site (TSS) of *cdh5* gene between the *cdh5* promoter region (P) and a putative enhancer (E) distant of ~20kb as defined by the presence of two ATAC-seq positive regions (Fig. S2 A, Fig. 5A) (Quillien et al. 2017, Bussmann et al. 2011). Therefore, in double transgenic individuals, the level of GFP fluorescence intensity correlates with endogenous *cdh5* expression. We also generated a transgenic line where the two ATAC-seq identified regions of *cdh5* were cloned next to each other, both upstream of the *Gal4VP16* coding sequence (Fig. 5E). In double transgenic embryos *Tg(cdh5:Gal4VP16); Tg(UAS:KAEDE),* the fluorescence intensity of the protein KAEDE was an artificial read out of *cdh5* transcription for which chromatin looping would not be needed. Comparing the level of fluorescence intensity in *TgBAC(cdh5:GAL4FF);Tg(UAS:GFP)* transgenic line in control condition or in the context of *prmt5* knock down, we observed a strong reduction of GFP fluorescence intensity in *prmt5* morphants (Fig. 5B-D), indicating that in an endogenous context Prmt5 was required for *cdh5* expression. In double transgenic embryos *Tg(cdh5:Gal4VP16); Tg(UAS:KAEDE)*, the fluorescent protein KAEDE was expressed in blood vessels (Fig. 5F), validating that the putative enhancer and the promotor region of *cdh5* are sufficient to drive gene expression in endothelial cells. However, in this artificial context, *prmt5* morpholino injection had no effect on the level of KAEDE fluorescence intensity as compared to control morphants (Fig. 5F-H). This result suggests that in this particular context *i.e* when chromatin looping between enhancer and promotor was not needed, Prmt5 was not required either for gene expression. This finding supports the idea that Prmt5 may play a role in the formation of the correct 3D environment for endothelial specific gene expression. Finally, rescue experiments were performed by injecting either wild type or a catalytic mutant of human *prmt5* mRNA to determine whether Prmt5 methyltransferase activity was required for the transcriptional control of *cdh5* expression in the endogenous context. We found that both wild type and mutant *hprmt5* mRNAs restored GFP fluorescence intensity in *prmt5* morphants as compared to control embryos (Fig. 5B-D, I-J). Collectively, these data indicate that the

transcriptional control of *cdh5* is likely independent of the Prmt5 methyltransferase activity and could rely on a role of Prmt5 as a scaffold protein to provide a proper chromatin conformation context.

DISCUSSION

Here we have demonstrated a role for Prmt5 in both hematopoiesis and blood vessel formation. Prmt5 promotes vascular morphogenesis through the transcriptional control of ETS transcription factor and adhesion proteins in endothelial cells. Intriguingly, we have shown that the methyltransferase activity of Prmt5 was not absolutely required to regulate gene expression, leading us to propose a role of scaffold protein for Prmt5 to facilitate chromatin looping formation in endothelial cells.

We found that similarly to Prmt5 in mouse (Liu et al 2015), Prmt5 plays an important role in zebrafish hematopoiesis by controlling HSCs emergence and HSPCs expansion. We also described for the first time the involvement of Prmt5 in vascular morphogenesis by regulating the expression of known genes that control this process (adhesion proteins or transcription factors) and *prmt5* loss of function partially phenocopied loss of function of these genes. Indeed, knocking down ETS protein alone had limited effect on sprout formation, while the combination of morpholinos against both *fli1a and fli1b,* and *ets1* led to a decreased number of vessel sprouts at 24 hpf but to a normal trunk vasculature at 48 hpf (Pham et al. 2007). Moreover, *amolt2a* knock down in zebrafish led to a reduced diameter of the DA in a similar way as we found in the context of *prmt5* loss of function (Hultin et al, 2014). Furthermore, previous studies have shown that loss of function of both *cdh5* and *esama* phenocopied what we observed in *prmt5* mutant *i.e* a disconnected stalk and tip cells and delayed formation of the DLAV formation (Sauteur et al. 2014, Sauteur et al. 2017). However, the loss of function of *cdh5* had no effect on HSCs emergence or HSPCs expansion (Anderson et al. 2015), suggesting that Prmt5 might act on different set of genes in endothelial cells and in emerging HSCs. In agreement with this hypothesis, Tan et al have proposed that Prmt5 is playing a

critical role in HSC quiescence through the splicing of genes involved in DNA repair (Tan et al 2019).

Interestingly, *prmt5* mutant and the mutant for the master regulator *etv2* shared similarities in their phenotypes such as an abnormal vasculature at 48 hpf characterized by a lack of lumen formation, a lack of vessel extension and aberrant connections (Pham et al. 2007, Craig et al. 2015). Similarly to the dynamics of *etv2* expression, single cell data analyses from Wagner et al. revealed that Prmt5 was expressed early in endothelial cells and that its expression decreased through time, and preceded the expression of ETV2 target genes (Wong et al., 2009, Wagner et al. 2018, Moore et al., 2013). However, we have shown that Prmt5 did not modify *etv2* expression while affecting ETV2 target genes, suggesting that Prmt5 instead of controlling *etv2* expression, could potentiate ETV2 activity through its methylation or through other mechanisms such as facilitation of ATP-dependent chromatin-remodeling complexes recruitments.

Prmt5 has been described to facilitate ATP-dependent chromatin remodeling to promote gene expression in skeletal muscle and during adipocyte differentiation (Dacwag et al, 2009, Leblanc et al. 2016, Leblanc et al. 2012, Pal et al.2013). Here, we proposed that Prmt5 could also be essential for proper chromatin looping in endothelial cells. Prmt5 influences gene expression only in an endogenous context where chromatin looping is required, while it is dispensable for gene expression when enhancer and promotor regions are artificially associated. This implies that Prmt5 could interact with Brg1 ATPase of SWI/SNF chromatin remodeling complex and with the mediator complex in endothelial cells as it does in muscle cells and adipocytes. Consistent with this hypothesis, *brg1* mutant mouse embryos display an anemia coupled to vascular defects in the yolk sac, characterized by thin vessels and supernumerary sprouts (Griffin et al. 2008), similarly to our present findings in zebrafish *prmt5* mutant. Interestingly, it has been proposed that the mediator complex regulates endothelial cell differentiation (Napoli et al. 2019) and the loss of *med12* subunit function in zebrafish leads to hematopoietic defects including a lack of lymphoid HSPC expansion (Keightley et al. 2011).

The presence of Prmt5 and Brg1 at promotor region of the *PPARγ2* locus or of *myogenin* was associated with dimethylation of H3R8 (histone 3 arginine 8) (Leblanc et al. 2012, Dacwag et al. 2007) with *prmt5* knock down leading to a reduction of both histone methylation and chromatin looping formation. *In vitro*, the addition of Prmt5 to Brg1 immunopurified complexes enhanced histone methylation, while the addition of a catalytic dead version of Prmt5 did not (Pal et al. 2003). Altogether those data suggest that wild type Prmt5, when recruited to target gene promoter regions, acts most likely by dimethylating histone proteins. However, these studies did not assess the ability of Prmt5 to facilitate chromatin looping independently (or not) of its methyltransferase activity. Our data suggest that chromatin looping favored by Prmt5 did not necessarily require its methyltransferase activity. Indeed, rescue experiments demonstrated that Prmt5 was able to restore gene expression independently of its catalytic domain, with the exception of *fli1a* expression. Of note, *fli1a* putative enhancer is located only 700 pb from the promotor region, suggesting that chromatin looping might not be required for *fli1a* expression, explaining the incapacity of the mutant form of Prmt5 to rescue *fli1a* expression. This data also indicates that depending on the context and the target genes considered, Prmt5 could modulate gene expression in endothelial cell through promotion of chromatin interaction but also probably *via* histones/proteins modification.

In conclusion, our study reveals a potential role of Prmt5 in promoting proper chromatin interaction in endothelial cell, and thus differentiation of these cells, as demonstrated during myogenesis and adipocyte differentiation. The role of Prmt5 in chromatin looping appears to be widespread in more cell types than originally thought and may be a pervasive role of Prmt5 during early development that is independent of its methyltransferase activity.

MATERIALS AND METHODS

Zebrafish care and maintenance

Embryos were raised and staged according to standard protocols (Kimmel et al., 1995). The establishment and characterization of Tg(gata2b:Gal4;UAS:lifeactGFP), Tg(fli1a:eGFP),

Tg(TP1bglob:VenusPEST)s940, TgBAC(cdh5:GAL4FF);Tg(UAS:GFP), Tg(UAS:KAEDE) have been described elsewhere (Butko et al. 2015; Lawson and Weinstein 2002; Ninov et al, 2012; Bussmann et al. 2011; Hatta et al. 2006). Lines generated in this study are described below. Embryos were fixed overnight at 4°C in BT-FIX, after which they were immediately processed or dehydrated and stored at −20°C until use.

Ethics statement

Fish were handled in a facility certified by the French Ministry of Agriculture (approval number A3155510). The project has received an agreement number APAFIS#7124-20161 00517263944 v3. Anesthesia and euthanasia procedures were performed in Tricaine Methanesulfonate (MS222) solutions as recommended for zebrafish (0.16 mg/ml for anesthesia, 0.30 mg/ml for euthanasia). All efforts were made to minimize the number of animals used and their suffering, in accordance with the guidelines from the European directive on the protection of animals used for scientific purposes (2010/63/UE) and the guiding principles from the French Decret 2013–118.

Plasmid construction

To construct the transgene Tg(*cdh5:GAL4VP16*), we cloned the putative *cdh5* promotor (*cdh5*P) and enhancer (*cdh5*E) elements into pme_mcs and p5E_GGWDest+ (Addgene #49319) (Kwan et al., 2007; Kirchmaieret al., 2013) using XhoI, EcorI and BsaI to give pme_*cdh5*P and p5E_*cdh5*E, respectively. The Gal4VP16 sequence from pme_Gal4VP16 (Kwan et al., 2007) was then introduced on downstream of *cdh5*P into pme_*cdh5*P using BamH1 and SpeI. We next performed a multisite LR recombination reaction (Gateway LR Clonase II Enzyme mix, Invitrogen) using p5E_*cdh5*E, pme_*cdh5*P:Gal4VP16, with pminTol-R4-R2pA to give pminTol- *cdh5*E-*cdh5*P: Gal4VP16.

Generation of *prmt5-/-* mutants by CRISPR/cas9

The guide RNA (gRNA) was designed using CHOPCHOP CRISPR Design website (Montague et al. 2014). The designed oligos were annealed and ligated into the gRNA plasmid pDR274

after digestion of the plasmid with BsaI (NEB). The gRNA was prepared *in vitro* using the MEGAshortscript T7 transcription kit (Ambion) after linearizing the plasmid with DraI (NEB) (Talbot and Amacher, 2014) before being purified using illustra MicroSpin G-50 Columns (GE Healthcare). 1 nL of a solution containing 10µM EnGen Cas9 NLS (NEB) and 100 ng/µl of gRNA was injected at the one-cell stage. WT, heterozygous, and homozygous *prmt5* animals were identified by PCR.

Microinjections

The Tg(*cdh5:GAL4VP16*);Tg(*UAS:KAEDE*) line was generated using pminTol- *cdh5*E-*cdh5*P: Gal4VP16 by Tol2 transposition as described previously (Covassin et al., 2009). Control and *prmt5* morpholino oligonucleotides (MOs) were described previously (Batut et al., 2011). Embryos from in-crosses of the indicated heterozygous carriers or wild-type adults were injected at the one- to two-cell stage with 6 ng of MO. pBluescript II KS+ hPRMT5 WT and pBluescript II KS+ hPRMT5 Mutant (Pal et al., 2003) were linearized by EcorI (NEB) and transcribed by T7 (Promega). 200 pg *hprmt5WT* mRNA, or *hprmt5 MUT* mRNA were injected at one cell stage.

RNA extraction, Reverse transcription and real-time PCR

Embryos were dissected at the indicated stage after addition of Tricaine Methanesulfonate. Genomic DNA was extracted from dissected embryo heads to identify their genotype and the corresponding dissected tails were conserved in TRIzol Reagent at -20°C. After identification of wild type and mutant embryos, total RNAs from at least 6 identified tails were extracted following manufacturer's instructions (Invitrogen). Total RNAs were converted into cDNA using Prime Script cDNA Synthesis Kit (Takara) with Oligo(dT) and random hexamer primers for 15 min at 37 °C according to manufacturer's instructions. cDNAs were then diluted 20-fold and quantified by qPCR using SsoFast Evagreen Supermix (Bio-rad) and specific primers. Data were acquired on CFX96 Real-Time PCR detection System (Bio-rad). Samples were analyzed

in triplicates and the expression level was calculated relative to zebrafish house keeping gene *EF1α*.

Live imaging

For the transgenic lines *TgBAC(cdh5:GAL4FF);*Tg(*UAS:GFP*) and Tg(*cdh5:GAL4VP16*);Tg(*UAS:KAEDE*), embryos were placed in 1.5% low melt agarose with Tricaine on a glass-bottomed culture dish filled with egg water. Images were acquired using the confocal microscope TCS SP8 (Leica Microsystems) with an L 25 × /0.95 W FLUOSTAR VIZIR objective (zoom X1.25) using the scanner resonant mode. Confocal stacks were acquired every 10 min from 28 to 38 hpf to generate movies.

Immunostaining

After fixation or rehydratation, embryos were washed twice with Phosphate Buffered Saline/1% Triton X-100 (PBST), permeabilized with PBST/0.5% Trypsin for 30 sec and washed twice again with PBST. After blocking with PBST/10% Fetal Calf Serum (FCS)/1% bovine serum albumin (BSA) (hereafter termed 'blocking solution') for at least 1 h, embryos were incubated with antibodies directed against either GFP (Torrey Pine, Biolabs), or Prmt5 (Upstate 07405), in blocking solution overnight at 4 °C followed by 5 washing steps with PBST. Embryos were then incubated with the appropriate Alexa Fluor-conjugated secondary antibodies (Molecular Probes) for at least 2 h at room temperature and washed three times. Nuclei were then stained with TO-PRO3 (Molecular Probes) and washed twice with PBST. Embryos were dissected, flat-mounted in glycerol and images were recorded on a confocal microscope as above.

Image processing and measurements

Confocal images and stacks were either analyzed with ImageJ software or LAS X. Nuclei of ISV cells and gata2b+ cells were counted using the Multipoint tool of ImageJ. ISV lengths were measured by drawing a line between the base and the tip of ISV on ImageJ. Contours of the Dorsal Aorta were drawn using the Freehand Selection Tool with a digital pen and the area

was then measured. Fluorescence intensity corresponded to the measurement of average gray value for each entire image.

Statistical analysis

Statistical comparisons of datasets were performed using GraphPad Prism software. For each dataset, we tested the assumption of normality with D'Agostino-Pearson tests and accordingly, unpaired t-test, Mann-Whitney test, One-way ANOVA, two-way ANOVA or Kruskal-Wallis test were used to compare dataset; means (± SEM) are indicated as horizontal bars on dot plots. The test used as well as the number of independent experiments performed and the minimal number of biological replicates are indicated in each figure legend.

Name/application	Sequence 5'-3'
sgRNA1-*zPrmt5*-FWD	TAGGGGTGGAACAGCGGCATACAC
sgRNA1-*zPrmt5*-REV	AAACGTGTATGCCGCTGTTCCACC
genotyping-*zPrmt5*-FWD	CAAGACCTGTCCTGTTTGATGA
genotyping-*zPrmt5*-REV	GTGACTTTGCAGGGTCCAGT
XhoI-promo*cdh5*-FWD	CCGCTCGAGCCAGGGGCATTTATCTTGG
EcorI-promo*cdh5*-REV	CGGAATTCAACGATCGCATACCAGAGT
BsaI-distenh*cdh5*-FWD	GTAACGGGTCTCCATGGGACAACAGTCAAAATGTAGCA
BsaI-distenh*cdh5*-REV	GTAACGGGTCTCCCTTACACTCGCATAACAATTTCCA
BamHI-*gal4VP16*-FWD	CGGGATCCGCCACCATGAAGCTACTGTCTTCTATC
SpeI-*gal4VP16*-REV	GGACTAGTCTACATATCCAGAGCGCCG
scla-qPCR-FWD	ATGGATGACCCTCCACAAAA
scla-qPCR-REV	TCCCGGTTTAGCTTCTCATC
runx1-qPCR-FWD	ACACTGGCGCTGCAACAAG
runx1-qPCR-REV	CATCATTTCCCGCCATCACT
cmyb-qPCR-FWD	GAACGGCTACGGTGGCTGGAA
cmyb-qPCR-REV	CAGAGTCCAGCGAAGGACTGT
EF1α-qPCR-FWD	GCATACATCAAGAAGATCGGC
EF1α-qPCR-REV	GCAGCCTTCTGTGCAGACTTTG
agtr2-qPCR-FWD	GTCATGTGCAAGCTGTGTGG
agtr2-qPCR-REV	AACACATGAACCAACCGGCC
esama-qPCR-FWD	AGACACCGAGGAGGATCTGG
esama-qPCR-REV	GCTGGGTTGGTGTTGTATCC
amotl2a-qPCR-FWD	GGGCACTTTATGCTCAACTCTTG
amotl2a-qPCR-REV	CGGCCTTGCTCTCGTCTT
fli1b-qPCR-FWD	TTCCATCAGCAGTCGTCTTG
fli1b-qPCR-REV	TAGTTCCCTCCCAGGTGATG
etv2-qPCR-FWD	TGCCTTTGGAGGAAGAAAGA

etv2-qPCR-REV	CTGTTGTTGGCAATCTGCTG
cdh5-qPCR-FWD	CGAGATTGCTGATGGAGGAACGCC
cdh5-qPCR-REV	TGGCGAGGAGGGCACTGACA
fli1a-qPCR-FWD	CCAAACATGACGACCAATGAGA
fli1a-qPCR-REV	GTGATCCGGAGACCACAGAGA

ACKNOWLEDGEMENTS

We would like to thank the Blader lab for helpful discussions and support; Dr. Cau, and Dr. Male and Dr. Navajas Acedo for critical reading of the manuscript; Aurore Laire for excellent zebrafish care; the Toulouse Rio Imaging (TRI) platform; Dr. Herbomel for the Zebrafish transgenic line *Tg(gata2b:Gal4;UAS:lifeactGFP).* This work was supported by a grant from the Fondation de l'Association pour la Recherche contre le Cancer (Fondation ARC) and from the Association Française contre les Myopathies (AFM) to LV. AQ was supported by a fellowship from the Fondation ARC.

COMPETING INTEREST

The authors declare no competing interests.

REFERENCES

Batut, J., C. Duboe, and L. Vandel. "The Methyltransferases Prmt4/Carm1 and Prmt5 Control Differentially Myogenesis in Zebrafish." *PLoS One* 6, no. 10 (2011): e25427.

Blanc, R. S., and S. Richard. "Arginine Methylation: The Coming of Age." *Mol Cell* 65, no. 1 (Jan 5 2017): 8-24.

Bussmann, J., and S. Schulte-Merker. "Rapid Bac Selection for Tol2-Mediated Transgenesis in Zebrafish." *Development* 138, no. 19 (Oct 2011): 4327-32.

Butko, E., M. Distel, C. Pouget, B. Weijts, I. Kobayashi, K. Ng, C. Mosimann*, et al.* "Gata2b Is a Restricted Early Regulator of Hemogenic Endothelium in the Zebrafish Embryo." *Development* 142, no. 6 (Mar 15 2015): 1050-61.

Carmeliet, P., V. Ferreira, G. Breier, S. Pollefeyt, L. Kieckens, M. Gertsenstein, M. Fahrig*, et al.* "Abnormal Blood Vessel Development and Lethality in Embryos Lacking a Single Vegf Allele." *Nature* 380, no. 6573 (Apr 4 1996): 435-9.

Covassin, L. D., A. F. Siekmann, M. C. Kacergis, E. Laver, J. C. Moore, J. A. Villefranc, B. M. Weinstein, and N. D. Lawson. "A Genetic Screen for Vascular Mutants in Zebrafish Reveals Dynamic Roles for Vegf/Plcg1 Signaling During Artery Development." *Dev Biol* 329, no. 2 (May 15 2009): 212-26.

Covassin, L. D., J. A. Villefranc, M. C. Kacergis, B. M. Weinstein, and N. D. Lawson. "Distinct Genetic Interactions between Multiple Vegf Receptors Are Required for Development of Different Blood Vessel Types in Zebrafish." *Proc Natl Acad Sci U S A* 103, no. 17 (Apr 25 2006): 6554-9.

Craig, M. P., V. Grajevskaja, H. K. Liao, J. Balciuniene, S. C. Ekker, J. S. Park, J. J. Essner, D. Balciunas, and S. Sumanas. "Etv2 and Fli1b Function Together as Key Regulators of Vasculogenesis and Angiogenesis." *Arterioscler Thromb Vasc Biol* 35, no. 4 (Apr 2015): 865-76.

Dacwag, C. S., M. T. Bedford, S. Sif, and A. N. Imbalzano. "Distinct Protein Arginine Methyltransferases Promote Atp-Dependent Chromatin Remodeling Function at Different Stages of Skeletal Muscle Differentiation." *Mol Cell Biol* 29, no. 7 (Apr 2009): 1909-21.

Fish, J. E., M. Cantu Gutierrez, L. T. Dang, N. Khyzha, Z. Chen, S. Veitch, H. S. Cheng*, et al.* "Dynamic Regulation of Vegf-Inducible Genes by an Erk/Erg/P300 Transcriptional Network." *Development* 144, no. 13 (Jul 1 2017): 2428-44.

Griffin, C. T., J. Brennan, and T. Magnuson. "The Chromatin-Remodeling Enzyme Brg1 Plays an Essential Role in Primitive Erythropoiesis and Vascular Development." *Development* 135, no. 3 (Feb 2008): 493-500.

Hatta, K., H. Tsujii, and T. Omura. "Cell Tracking Using a Photoconvertible Fluorescent Protein." *Nat Protoc* 1, no. 2 (2006): 960-7.

Hultin, S., Y. Zheng, M. Mojallal, S. Vertuani, C. Gentili, M. Balland, R. Milloud*, et al.* "Amotl2 Links Ve-Cadherin to Contractile Actin Fibres Necessary for Aortic Lumen Expansion." *Nat Commun* 5 (May 7 2014): 3743.

Kalna, V., Y. Yang, C. R. Peghaire, K. Frudd, R. Hannah, A. V. Shah, L. Osuna Almagro*, et al.* "The Transcription Factor Erg Regulates Super-Enhancers Associated with an Endothelial-Specific Gene Expression Program." *Circ Res* 124, no. 9 (Apr 26 2019): 1337-49.

Karkhanis, V., Y. J. Hu, R. A. Baiocchi, A. N. Imbalzano, and S. Sif. "Versatility of Prmt5-Induced Methylation in Growth Control and Development." *Trends Biochem Sci* 36, no. 12 (Dec 2011): 633-41.

Keightley, M. C., J. E. Layton, J. W. Hayman, J. K. Heath, and G. J. Lieschke. "Mediator Subunit 12 Is Required for Neutrophil Development in Zebrafish." *PLoS One* 6, no. 8 (2011): e23845.

Kimmel, C. B., W. W. Ballard, S. R. Kimmel, B. Ullmann, and T. F. Schilling. "Stages of Embryonic Development of the Zebrafish." *Dev Dyn* 203, no. 3 (Jul 1995): 253-310.

Kirchmaier, S., K. Lust, and J. Wittbrodt. "Golden Gateway Cloning--a Combinatorial Approach to Generate Fusion and Recombination Constructs." *PLoS One* 8, no. 10 (2013): e76117.

Kwan, K. M., E. Fujimoto, C. Grabher, B. D. Mangum, M. E. Hardy, D. S. Campbell, J. M. Parant*, et al.* "The Tol2kit: A Multisite Gateway-Based Construction Kit for Tol2 Transposon Transgenesis Constructs." *Dev Dyn* 236, no. 11 (Nov 2007): 3088-99.

Lawson, N. D., and B. M. Weinstein. "In Vivo Imaging of Embryonic Vascular Development Using Transgenic Zebrafish." *Dev Biol* 248, no. 2 (Aug 15 2002): 307-18.

LeBlanc, S. E., S. Konda, Q. Wu, Y. J. Hu, C. M. Oslowski, S. Sif, and A. N. Imbalzano. "Protein Arginine Methyltransferase 5 (Prmt5) Promotes Gene Expression of Peroxisome Proliferator-Activated Receptor Gamma2 (Ppargamma2) and Its Target Genes During Adipogenesis." *Mol Endocrinol* 26, no. 4 (Apr 2012): 583-97.

LeBlanc, S. E., Q. Wu, P. Lamba, S. Sif, and A. N. Imbalzano. "Promoter-Enhancer Looping at the Ppargamma2 Locus During Adipogenic Differentiation Requires the Prmt5 Methyltransferase." *Nucleic Acids Res* 44, no. 11 (Jun 20 2016): 5133-47.

Liu, F., G. Cheng, P. J. Hamard, S. Greenblatt, L. Wang, N. Man, F. Perna*, et al.* "Arginine Methyltransferase Prmt5 Is Essential for Sustaining Normal Adult Hematopoiesis." *J Clin Invest* 125, no. 9 (Sep 2015): 3532-44.

Liu, F., D. Li, Y. Y. Yu, I. Kang, M. J. Cha, J. Y. Kim, C. Park*, et al.* "Induction of Hematopoietic and Endothelial Cell Program Orchestrated by Ets Transcription Factor Er71/Etv2." *EMBO Rep* 16, no. 5 (May 2015): 654-69.

Ma, D., Y. Wei, and F. Liu. "Regulatory Mechanisms of Thymus and T Cell Development." *Dev Comp Immunol* 39, no. 1-2 (Jan-Feb 2013): 91-102.

Mans, B. J., J. F. Andersen, I. M. Francischetti, J. G. Valenzuela, T. G. Schwan, V. M. Pham, M. K. Garfield, C. H. Hammer, and J. M. Ribeiro. "Comparative Sialomics between Hard and Soft

Ticks: Implications for the Evolution of Blood-Feeding Behavior." *Insect Biochem Mol Biol* 38, no. 1 (Jan 2008): 42-58.

Montague, T. G., J. M. Cruz, J. A. Gagnon, G. M. Church, and E. Valen. "Chopchop: A Crispr/Cas9 and Talen Web Tool for Genome Editing." *Nucleic Acids Res* 42, no. Web Server issue (Jul 2014): W401-7.

Moore, J. C., S. Sheppard-Tindell, I. A. Shestopalov, S. Yamazoe, J. K. Chen, and N. D. Lawson. "Post-Transcriptional Mechanisms Contribute to Etv2 Repression During Vascular Development." *Dev Biol* 384, no. 1 (Dec 1 2013): 128-40.

Napoli, C., C. Schiano, and A. Soricelli. "Increasing Evidence of Pathogenic Role of the Mediator (Med) Complex in the Development of Cardiovascular Diseases." *Biochimie* 165 (Oct 2019): 1-8.

Ninov, N., M. Borius, and D. Y. Stainier. "Different Levels of Notch Signaling Regulate Quiescence, Renewal and Differentiation in Pancreatic Endocrine Progenitors." *Development* 139, no. 9 (May 2012): 1557-67.

Pal, S., R. Yun, A. Datta, L. Lacomis, H. Erdjument-Bromage, J. Kumar, P. Tempst, and S. Sif. "Msin3a/Histone Deacetylase 2- and Prmt5-Containing Brg1 Complex Is Involved in Transcriptional Repression of the Myc Target Gene Cad." *Mol Cell Biol* 23, no. 21 (Nov 2003): 7475-87.

Pham, V. N., N. D. Lawson, J. W. Mugford, L. Dye, D. Castranova, B. Lo, and B. M. Weinstein. "Combinatorial Function of Ets Transcription Factors in the Developing Vasculature." *Dev Biol* 303, no. 2 (Mar 15 2007): 772-83.

Quillien, A., M. Abdalla, J. Yu, J. Ou, L. J. Zhu, and N. D. Lawson. "Robust Identification of Developmentally Active Endothelial Enhancers in Zebrafish Using Fans-Assisted Atac-Seq." *Cell Rep* 20, no. 3 (Jul 18 2017): 709-20.

Quillien, A., J. C. Moore, M. Shin, A. F. Siekmann, T. Smith, L. Pan, C. B. Moens, M. J. Parsons, and N. D. Lawson. "Distinct Notch Signaling Outputs Pattern the Developing Arterial System." *Development* 141, no. 7 (Apr 2014): 1544-52.

Rosa-Garrido, M., D. J. Chapski, and T. M. Vondriska. "Epigenomes in Cardiovascular Disease." *Circ Res* 122, no. 11 (May 25 2018): 1586-607.

Sauteur, L., M. Affolter, and H. G. Belting. "Distinct and Redundant Functions of Esama and Ve-Cadherin During Vascular Morphogenesis." *Development* 144, no. 8 (Apr 15 2017): 1554-65.

Sauteur, L., A. Krudewig, L. Herwig, N. Ehrenfeuchter, A. Lenard, M. Affolter, and H. G. Belting. "Cdh5/Ve-Cadherin Promotes Endothelial Cell Interface Elongation Via Cortical Actin Polymerization During Angiogenic Sprouting." *Cell Rep* 9, no. 2 (Oct 23 2014): 504-13.

Shailesh, H., Z. Z. Zakaria, R. Baiocchi, and S. Sif. "Protein Arginine Methyltransferase 5 (Prmt5) Dysregulation in Cancer." *Oncotarget* 9, no. 94 (Nov 30 2018): 36705-18.

Shalaby, F., J. Ho, W. L. Stanford, K. D. Fischer, A. C. Schuh, L. Schwartz, A. Bernstein, and J. Rossant. "A Requirement for Flk1 in Primitive and Definitive Hematopoiesis and Vasculogenesis." *Cell* 89, no. 6 (Jun 13 1997): 981-90.

Stopa, N., J. E. Krebs, and D. Shechter. "The Prmt5 Arginine Methyltransferase: Many Roles in Development, Cancer and Beyond." *Cell Mol Life Sci* 72, no. 11 (Jun 2015): 2041-59.

Talbot, J. C., and S. L. Amacher. "A Streamlined Crispr Pipeline to Reliably Generate Zebrafish Frameshifting Alleles." *Zebrafish* 11, no. 6 (Dec 2014): 583-5.

Tan, D. Q., Y. Li, C. Yang, J. Li, S. H. Tan, D. W. L. Chin, A. Nakamura-Ishizu, H. Yang, and T. Suda. "Prmt5 Modulates Splicing for Genome Integrity and Preserves Proteostasis of Hematopoietic Stem Cells." *Cell Rep* 26, no. 9 (Feb 26 2019): 2316-28 e6.

Tee, W. W., M. Pardo, T. W. Theunissen, L. Yu, J. S. Choudhary, P. Hajkova, and M. A. Surani. "Prmt5 Is Essential for Early Mouse Development and Acts in the Cytoplasm to Maintain Es Cell Pluripotency." *Genes Dev* 24, no. 24 (Dec 15 2010): 2772-7.

Wagner, D. E., C. Weinreb, Z. M. Collins, J. A. Briggs, S. G. Megason, and A. M. Klein. "Single-Cell Mapping of Gene Expression Landscapes and Lineage in the Zebrafish Embryo." *Science* 360, no. 6392 (Jun 1 2018): 981-87.

Wong, K. S., K. Proulx, M. S. Rost, and S. Sumanas. "Identification of Vasculature-Specific Genes by Microarray Analysis of Etsrp/Etv2 Overexpressing Zebrafish Embryos." *Dev Dyn* 238, no. 7 (Jul 2009): 1836-50.

Zhu, J., D. Zhang, X. Liu, G. Yu, X. Cai, C. Xu, F. Rong*, et al.* "Zebrafish Prmt5 Arginine Methyltransferase Is Essential for Germ Cell Development." *Development* 146, no. 20 (Oct 14 2019).

FIGURE LEGENDS

Figure 1: Loss of *prmt5* affect HSCs and HSPCs production. A- Schematic representation of the sequence targeted by CRISPR/Cas9 leading to a 23 nucleotide deletion, and of wild type and truncated Prmt5 proteins. The catalytic domain “CAT” appears in magenta. **B**-**C**- Confocal section of immunostaining with anti-Prmt5 antibody of wild type and *prmt5* mutant embryos at 24 hpf. Scale bar 100 µm. **D**- Schematic representation of vascular (green) and hematopoietic (red) systems in a zebrafish larvae. Circle and bracket indicate the Thymus (T) and the Caudal Hematopoietic Tissue (CHT), respectively. **D’**- Close-up of the trunk vasculature where HSCs emerge from the ventral wall of the dorsal aorta (DA), bud and migrate. Red line represents the diameter of the dorsal aorta. Cardinal Vein (CV). **E**-**F’**- Confocal section of transgenic *Tg*(*gata2b:Gal4; UAS:lifeactGFP*) embryos at 36 hpf showing gata2b+ cells in red and TO-PRO-3 in black. Blue arrows indicate HSCs labelled in red in wild type (**E**, **E’**) and in *prmt5* mutant (**F**, **F’**) embryos. Bar scale 100 µm. **G**- Average number of HSCs enumerated per confocal stack in wild type and in *prmt5* mutant embryos at 36 hpf. Data are from 3 independent experiments with at least 6 individuals per experiment and a Mann-Whitney test was performed. **H**- Relative mRNA expressions determined by RT-qPCR in 36 hpf wild type and *prmt5* mutant embryos, from 3 independent experiments with at least 6 animals per condition. Two way ANOVA was performed. **I**-**J**- Confocal section of wild type (**I**) and *prmt5* mutant (**J**) thymus from transgenic Tg(*gata2b:Gal4; UAS:lifeactGFP*) embryos at 5 days. Thymus are delimited by a white circle. Bar scale 100 µm. **K**- Average number of HSPCs enumerated per confocal stack in wild type and *prmt5* mutant embryos at 5 days from 3 independent experiments with at least 5 individuals per analysis. T-test was performed. * P<0.05, ** P<0.01, ***P<0.001.

Figure 2: Loss of *prmt5* impairs blood vessel formation. **A**-**C'**- Confocal projections of transgenic *Tg(fli1a:GFP)^{y1}* embryos with endothelial cells (in green) after immunostaining against Prmt5 (in magenta). **A**-**A''**- Dorsal view of the lateral plate mesoderm at 14 somites. Yellow rectangle delimits the close up of Prmt5+ endothelial cells (**A'**-**A''**). Prmt5+ cells appears in magenta (**A**-**A"**) and endothelial cells in green (**A**-**A'**). Anterior is on top. Scale bars 100 µm (**A**) and 25 µm (**A'**). **B**-**B'**- Confocal projection focusing on endothelial cells (in green) from the dorsal aorta (DA) and the cardinal vein (CV) at 24 hpf. Red and blue arrows point to Prmt5+ cells (in magenta) from the DA and the CV, respectively. Red and blue lines represent DA and CV diameters, respectively. Scale bar 50 µm. **C**-**C'**- Confocal projection focusing on sprouting ISVs (in green) at 24 hpf. Light blue and yellow arrows point to tip and stalk cell, respectively. **D**- Schematic representation of the trunk vasculature with ISVs sprouting from the DA. The tip cell leads the cell migration and the stalk cell maintains the connection with the DA. **E**-**F**- Confocal projection of transgenic *Tg(fli1a:GFP)^{y1}* wild type (**E**) and *prmt5* mutant (**F**) embryos at 28 hpf. Red rectangles delimit where DA close ups was made. White rectangles delimit the higher magnification (x2) of the DA with red lines indicating the dorsal aorta diameters. White arrows indicate the connection point between two ISVs to form the Dorsal Longitudinal Anastomotic Vessel (DLAV). Scale bar 100 µm. **G**-**H**- Confocal projections of control morphant (**G**) and *prmt5* morphant (**H**) transgenic *Tg(TP1bglob:VenusPEST)^{s940}* embryos labelling cells from the DA at 28 hpf. Yellow lines delimit the measured area occupied by the DA. Scale bar 25 µm **I**- Average area occupied by the DA in μm^2 in control and *prmt5* morpholino injected embryos from 2 independent experiments with at least 8 animals per condition. T-test was performed. **J**-**K**- Average number of endothelial cells per intersegmental vessel (**J**) and average ISV length in µm (**K**) in control and in *prmt5* mutant embryos from 3 independent experiments with at least 3 animals per condition. T-test and Mann Whitney test were performed, respectively. ** P<0.01, ***P<0.001.

Figure3: Prmt5 is required for vascular morphogenesis. A-**B**- Still images from Movies S1 and S2 from control (**A**) and *prmt5* morphant (**B**) Tg(fli1a:GFP)^{y1} transgenic embryos from 28

to 38 hpf. Red asterisks labelled missing connections between tip and stalk cells as well as missing connections between tip cells that should lead to DLAV formation. Red arrows point to connecting ISVs leading to DLAV formation. White arrows indicate supernumerary sprouts. Yellow asterisks label the lumen of ISVs. Scale bar 50 µm. **C**- Relative mRNA expressions of the indicated transcripts were determined by RT-qPCR in 28 hpf wild type and *prmt5* mutant embryos, from 3 independent experiments with at least 6 animals per condition. Two way ANOVA was performed. * P<0.05, ***P<0.001.

Figure 4: Prmt5 methyltransferase activity is dispensable for vascular morphogenesis. **A**-**D**- Confocal projection of transgenic *Tg*(*fli1a:GFP*)^{y1} embryos at 28 hpf. Wild type embryo is on the top left panel (**A**), *prmt5* mutant embryos were not injected (**B**) or injected with either *hprmt5WT* mRNA (**C**) or the mutant form *hprmt5MUT* mRNA (**D**). Scale bar 100 µm. **E**-**F**- Average ISVs length in µm (**E**) and average number of endothelial cells per ISVs (**F**) for wild type, *prmt5* mutant embryos not injected or injected with *hprmt5WT* mRNA, or *hprmt5 MUT* mRNA, from 3 independent experiments with at least 3 animals per condition. Kruskal-Wallis test (**E**) and One way ANOVA (**F**) were performed. ** P<0.01, *** P<0.001. **G**- Relative mRNA expressions were determined by RT-qPCR on 28 hpf wild type and *prmt5* mutant embryos injected by either *hprmt5WT or hprmt5MUT* mRNAs, from 2 independent experiments with at least 6 animals per condition. Two way ANOVA was performed. * P<0.05.

Figure 5: Prmt5 promotes chromatin looping. A- Schematic representation of the transgene *TgBAC(cdh5:GAL4FF)* containing two putative cis-regulatory elements, a promotor region (P) and an enhancer (E), separated by ~20kb with the *GAL4FF* reporter gene inserted at the TSS of *cdh5.* **B**, **C**, **I**, **J**- Confocal projections of transgenic *TgBAC(cdh5:GAL4FF);*Tg(*UAS:GFP*) embryos at 28 hpf. Control morphant is on the top left panel (**B**), *prmt5* morphant embryos were not injected (**C**) or injected by either *hprmt5WT* mRNA (**I**) or the catalytic mutant form *hprmt5MUT* (**J**) mRNA. The fluorescent intensity is colored coded, from the Low intensity (L) in black to High intensity (H) in white (intensity scale as in panel **B**). Scale bar 100 µm. **D**- Average GFP fluorescence intensity per confocal projection for control, *prmt5* morphant

embryos injected by *hprmt5WT* mRNA, or *hprmt5 MUT* mRNA or not injected, from 3 independent experiments with at least 3 animals per condition. One way ANOVA was performed. * P<0.05, **P<0.01. **E**- Schematic representation of the transgene Tg(*cdh5:GAL4VP16*) containing the two putative cis-regulatory elements next to each other (E and P), upstream of *GAL4VP16* reporter gene. **F**-**G**- Confocal projection of transgenic Tg(*cdh5:GAL4VP16*);Tg(*UAS:KAEDE*) embryos at 26 hpf injected with either a control morpholino (**F**) or *a prmt5* morpholino (**G**). The fluorescence intensity is color- coded, from the Low intensity (L) in black to High intensity (H) in white (intensity scale in panel **B**). **H**- Average KAEDE fluorescence intensity for control and for *prmt5* morphant embryos, from 3 independent experiments with at least 5 animals per condition. T-test was performed.

Figure S1: A-**B**- Confocal section of Prmt5 immunostaining in control and *prmt5* morphant embryos at 24 hpf. Scale bar 100 µm. **C**-**D**- Confocal projections of transgenic Tg(*fli1a:GFP*)^{y1} embryos injected by either control morpholino (**C**) or *prmt5* morpholino (**D**). **E**-**F**- Average number of endothelial cells per ISV (**E**) and average ISV length in µm (**F**), in control and *prmt5* morphant embryos, from 3 independent experiments with at least 4 animals per condition. T-test and Mann-Whitney test were performed. *** P<0.001.

Figure S2: Chromatin profile visualization of endothelial cells from the UCSC Genome Browser. ATAC-seq peaks as determined by Quillien et al. (Quillien et al. 2017) flanking indicated genes (*cdh5, esama, agtr2, fli1a, fli1b, amotl2a*). Promoter regions (P) and putative enhancers (E) are highlighted in light orange and light purple, respectively.

figure1

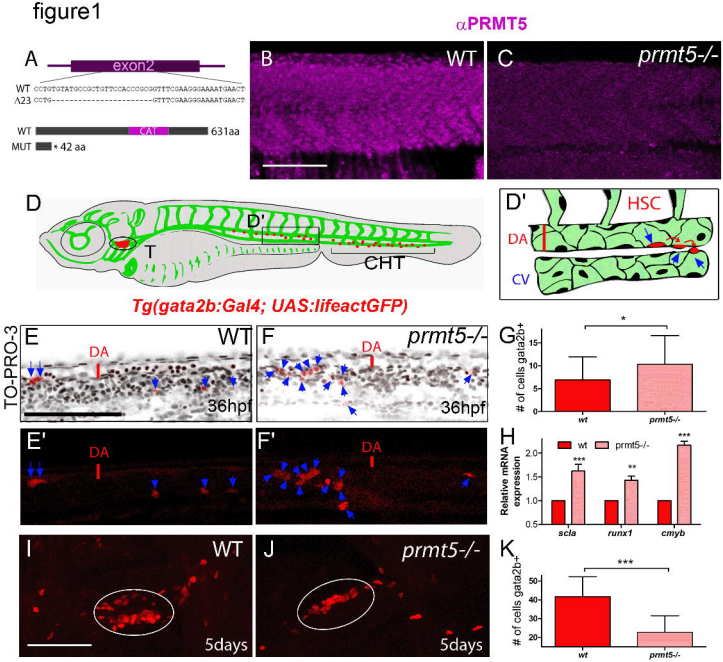
αPRMT5
A
exon2
WT CCTGTGTATGCCGCTGTTCCACCCGCGGTTTCGAAGGGAAAATGAACT
Δ23 CCTG----------GTTTCGAAGGGAAAATGAACT
WT
CAI
631aa
MUT
+ 42 aa
B
WT
C
prmt5-/-
D
D'
T
CHT
D'
HSC
DA
CV
Tg(gata2b:Gal4; UAS:lifeactGFP)
TO-PRO-3
E
WT
DA
36hpf
F
prmt5-/-
DA
36hpf
E'
DA
F'
DA
G
# of cells gata2b+
wt
prmt5-/-
H
wt
prmt5-/-
Relative mRNA expression
scla
runx1
cmyb
I
WT
5days
J
prmt5-/-
5days
K
# of cells gata2b+
wt
prmt5-/-

figure2

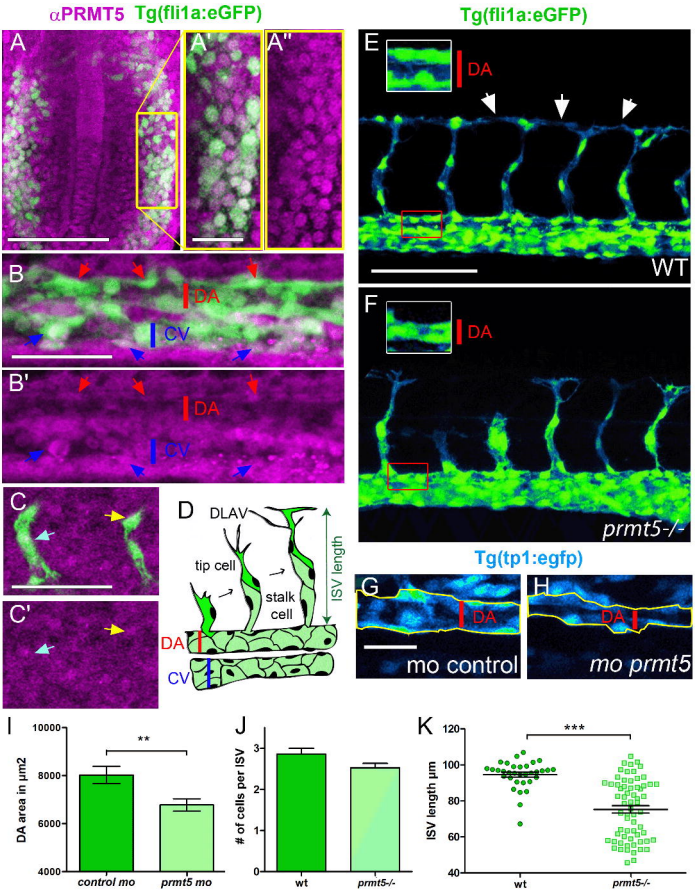
αPRMT5 Tg(fli1a:eGFP)
A
A'
A''
B
DA
CV
B'
DA
CV
C
C'
D
DLAV
tip cell
stalk cell
ISV length
DA
CV
Tg(fli1a:eGFP)
E
DA
WT
F
DA
prmt5-/-
Tg(tp1:egfp)
G
DA
mo control
H
DA
mo prmt5
I
DA area in µm2
10000
8000
6000
4000
**
control mo
prmt5 mo
J
# of cells per ISV
3
2
1
0
wt
prmt5-/-
K
ISV length µm
120
100
80
60
40
***
wt
prmt5-/-

figure3

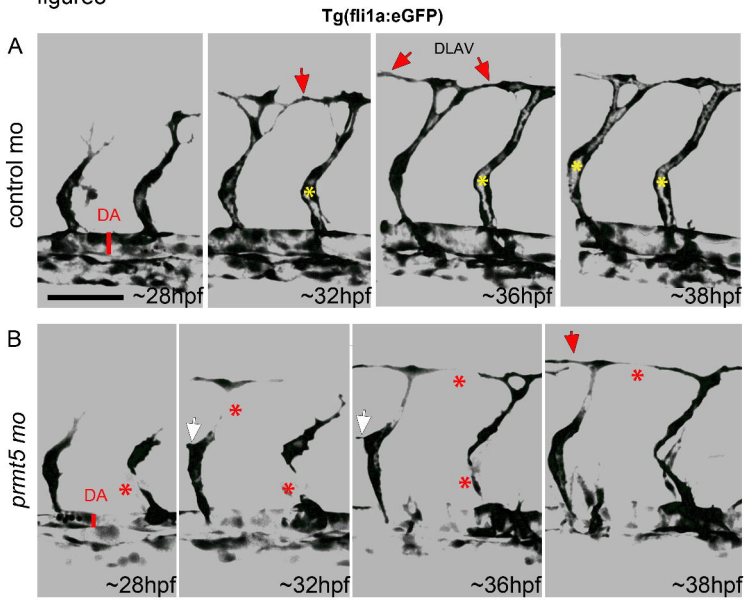
Tg(fli1a:eGFP)
A
control mo
DA
DLAV
~28hpf
~32hpf
~36hpf
~38hpf
B
prmt5 mo
DA
~28hpf
~32hpf
~36hpf
~38hpf

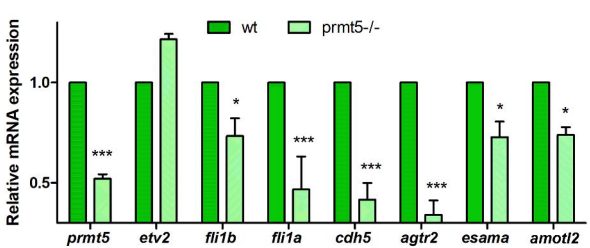
C
wt
prmt5-/-
Relative mRNA expression
1.0
0.5
***
*
prmt5
etv2
fli1b
fli1a
cdh5
agtr2
esama
amotl2

figure4

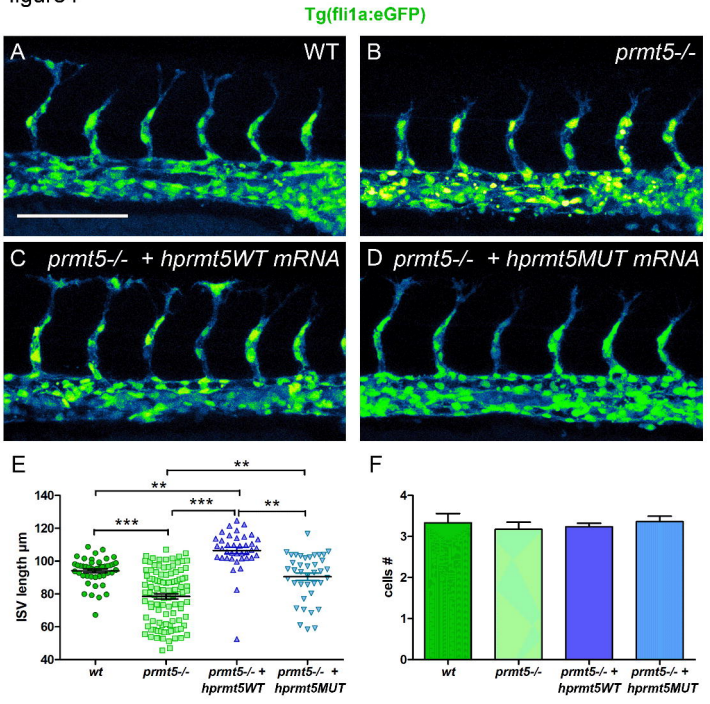
Tg(fli1a:eGFP)
A
WT
B
prmt5-/-
C
prmt5-/- + hprmt5WT mRNA
D
prmt5-/- + hprmt5MUT mRNA
E
ISV length µm
140
120
100
80
60
40
**
**
***
***
**
wt
prmt5-/-
prmt5-/- + hprmt5WT
prmt5-/- + hprmt5MUT
F
cells #
4
3
2
1
0
wt
prmt5-/-
prmt5-/- + hprmt5WT
prmt5-/- + hprmt5MUT
G
wt
prmt5-/- + hprmt5WT
prmt5-/- + hprmt5WT mRNA
Relative mRNA expression
1.5
1.0
0.5
0.0
*
fli1b
fli1a
cdh5
agtr2
esama
amotl2

figure5

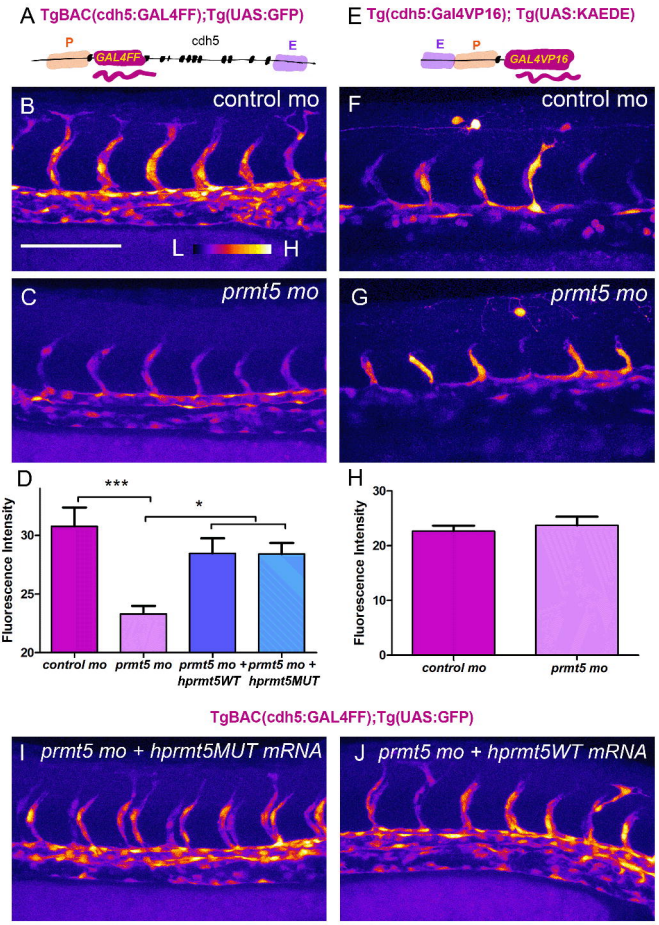
A TgBAC(cdh5:GAL4FF);Tg(UAS:GFP)
P
cdh5
E
GAL4FF
E Tg(cdh5:Gal4VP16); Tg(UAS:KAEDE)
E
P
GAL4VP16
B
control mo
L
H
F
control mo
C
prmt5 mo
G
prmt5 mo
D
***
*
Fluorescence Intensity
30
25
20
control mo
prmt5 mo
prmt5 mo + hprmt5WT
prmt5 mo + hprmt5MUT
H
Fluorescence Intensity
30
20
10
0
control mo
prmt5 mo
TgBAC(cdh5:GAL4FF);Tg(UAS:GFP)
I
prmt5 mo + hprmt5MUT mRNA
J
prmt5 mo + hprmt5WT mRNA

figureS1

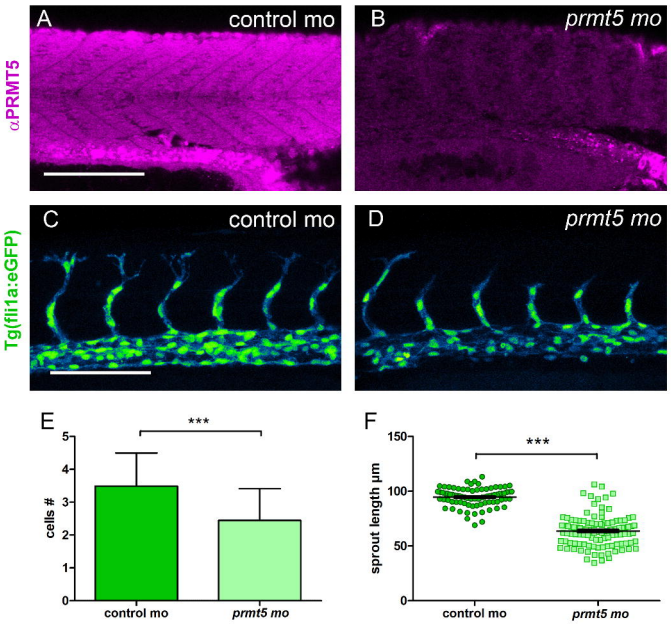
A
control mo
B
prmt5 mo
αPRMT5
C
control mo
D
prmt5 mo
Tg(fli1a:eGFP)
E
***
cells #
0
1
2
3
4
5
control mo
prmt5 mo
F
***
sprout length µm
0
50
100
150
control mo
prmt5 mo

figureS2

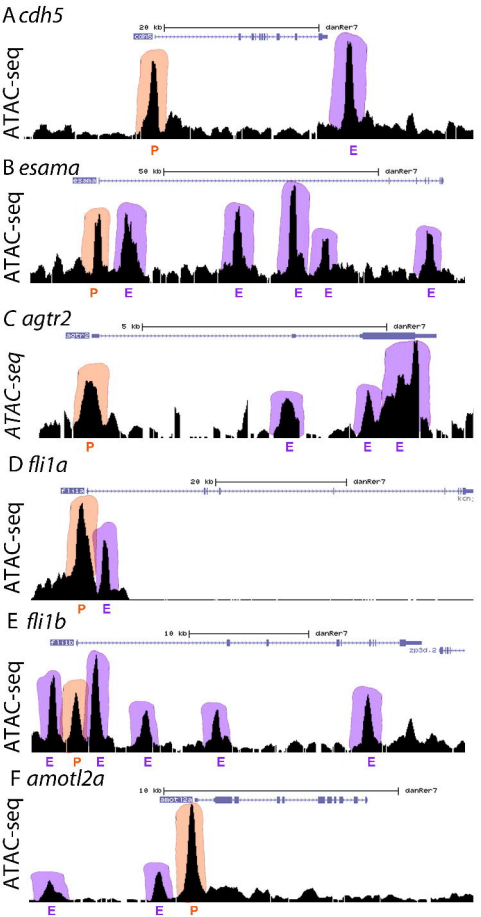
A cdh5
ATAC-seq
20 kb
danRer7
P
E
B esama
ATAC-seq
50 kb
danRer7
P
E
E
E
E
E
C agtr2
ATAC-seq
5 kb
danRer7
P
E
E
E
D fli1a
ATAC-seq
20 kb
danRer7
P
E
E fli1b
ATAC-seq
10 kb
danRer7
E
P
E
E
E
E
F amotl2a
ATAC-seq
10 kb
danRer7
E
E
P